







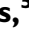









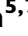


REPORT

A Māori specific *RFC1* pathogenic repeat configuration in CANVAS, likely due to a founder allele

 Sarah J. Beecroft,^{1,2,*}
 Andrea Cortese,^{3,4,*}
 Roisin Sullivan,^{3,#}
 Wai Yan Yau,^{3,#}
 Zoe Dyer,⁵
 Teddy Y. Wu,⁶
 Eoin Mulroy,⁵
 Luciana Pelosi,⁵
 Miriam Rodrigues,⁵
 Rachael Taylor,⁷
 Stuart Mossman,⁸
 Ruth Leadbetter,⁸
 James Cleland,⁹
 Tim Anderson,⁶
 Gianina Ravenscroft,^{1,2}
 Nigel G. Laing,^{1,2}
 Henry Houlden,³
 Mary M. Reilly³ and
  Richard H. Roxburgh^{5,7}

*,#These authors contributed equally to this work.

Cerebellar ataxia with neuropathy and bilateral vestibular areflexia syndrome (CANVAS) is a recently recognized neurodegenerative disease with onset in mid- to late adulthood. The genetic basis for a large proportion of Caucasian patients was recently shown to be the biallelic expansion of a pentanucleotide (AAGGG)_n repeat in *RFC1*. Here, we describe the first instance of CANVAS genetic testing in New Zealand Māori and Cook Island Māori individuals. We show a novel, possibly population-specific CANVAS configuration (AAAGG)₁₀₋₂₅(AAGGG)_{exp}, which was the cause of CANVAS in all patients. There were no apparent phenotypic differences compared with European CANVAS patients. Presence of a common disease haplotype among this cohort suggests this novel repeat expansion configuration is a founder effect in this population, which may indicate that CANVAS will be especially prevalent in this group. Haplotype dating estimated the most recent common ancestor at ~1430 CE. We also show the same core haplotype as previously described, supporting a single origin of the CANVAS mutation.

- 1 Neurogenetic Diseases Group, Centre for Medical Research, QEII Medical Centre, University of Western Australia, Nedlands, WA 6009, Australia
- 2 Harry Perkins Institute of Medical Research, QEII Medical Centre, Nedlands, WA 6009, Australia
- 3 Department of Neuromuscular Disease, UCL Queen Square Institute of Neurology and The National Hospital for Neurology and Neurosurgery, London, UK
- 4 Brain and Behavioural Sciences, University of Pavia, Pavia, Italy
- 5 Neurology Department, Auckland City Hospital, Auckland, New Zealand
- 6 Department of Neurology, Christchurch Hospital, Christchurch, New Zealand
- 7 Centre for Brain Research Neurogenetics Research Clinic, University of Auckland, Auckland, New Zealand
- 8 Neurology Department, Wellington Hospital, Wellington, New Zealand
- 9 Neurology Department, Tauranga Hospital, Tauranga, New Zealand

Correspondence to: Sarah J. Beecroft
 Harry Perkins Institute of Medical Research, QEII Medical Centre
 Nedlands, WA 6009, Australia
 E-mail: sarah.beecroft@uwa.edu.au

Received December 2, 2019. Revised April 12, 2020. Accepted May 7, 2020

© The Author(s) (2020). Published by Oxford University Press on behalf of the Guarantors of Brain. All rights reserved.

For permissions, please email: journals.permissions@oup.com

Correspondence may also be addressed to: Richard H. Roxburgh
Neurology Department, Auckland City Hospital
Private Bag 92024, Auckland, New Zealand
E-mail: RichardR@adhb.govt.nz

Keywords: CANVAS; repeat expansion; RFC1; founder effect; Māori

Abbreviations: CANVAS = cerebellar ataxia with neuropathy and bilateral vestibular areflexia syndrome; WGS = whole genome sequencing

Introduction

The combination of cerebellar ataxia, neuropathy, and bilateral vestibular areflexia was recently recognized as a distinct syndrome (CANVAS) (Szmulewicz *et al.*, 2011). This slowly progressive neurodegenerative disease usually presents in mid to late adulthood (>30 years) (Szmulewicz *et al.*, 2011). Additional features include chronic cough, autonomic dysfunction (Taylor *et al.*, 2014; Cortese *et al.*, 2019) and thinning of the peripheral nerves (Pelosi *et al.*, 2018). Striking neuropathological features include atrophy of the Purkinje cells; vestibular, geniculate and trigeminal ganglia; and dorsal root ganglia and posterior columns (Szmulewicz *et al.*, 2014). Cortese *et al.* (2019) showed that a recessive pentanucleotide repeat expansion is responsible for the vast majority of Caucasian cases and this has been confirmed in a second cohort from Australia (Rafehi *et al.*, 2019). The expansion occurs in the poly(A) tail of an AluSx3 element in intron two of *RFC1*. At this locus, the reference allele is (AAAAG)₁₁. Other benign configurations include (AAAAG)_{exp} and (AAAGG)_{exp}. The pathogenic CANVAS allele is estimated to be 400–2000 repeated units of AAGGG. The estimated carrier frequency of the pathogenic CANVAS allele is 0.7% in Caucasians, which would make CANVAS one of the most common hereditary forms of late-onset ataxia (Cortese *et al.*, 2019). However, this finding requires validation in other populations. We describe the first reported genetic characterization of CANVAS in New Zealand Māori and Cook Island Māori individuals, who comprise a significant part of the New Zealand/Cook Island population. CANVAS has been seen in this group previously (Taylor *et al.*, 2014). We show that these patients have a different conformation of the pathogenic pentanucleotide repeat.

Materials and methods

Cohort

This study was approved by the University of Western Australia Human Research Ethics Committee and the New Zealand Health and Disability Ethics Committee. DNA was obtained for 15 individuals; 13 were affected, and two were unaffected family members. All individuals gave informed consent for DNA collection and analysis, except Individual M2 III:2. Individual

M2 III:2 passed away prior to the study, and therefore informed consent was obtained from the patient's family to use a stored DNA sample. Affected individuals were recruited from neurology clinics in New Zealand. There were two multiplex families and five singleton patients (Fig. 1 and Table 1). Twelve individuals were Māori (M), and three were Cook Island Māori (CI). Five individuals (Individuals M3 I:1, M4 I:1, M5 I:1 M6 I:1 and M7 I:1) have been previously described clinically (Taylor *et al.*, 2014).

Clinical data collection

Apart from Individual M2 III:2, all affected individuals were clinically assessed at study recruitment. Follow-up information was taken from clinical documentation, phone interviews and follow-up examination of key affected individuals ($n = 13$). Contact was made with seven affected individuals. Four patients could not be contacted, and two affected individuals (Individuals M2 III:5 and M3 I:1) had died.

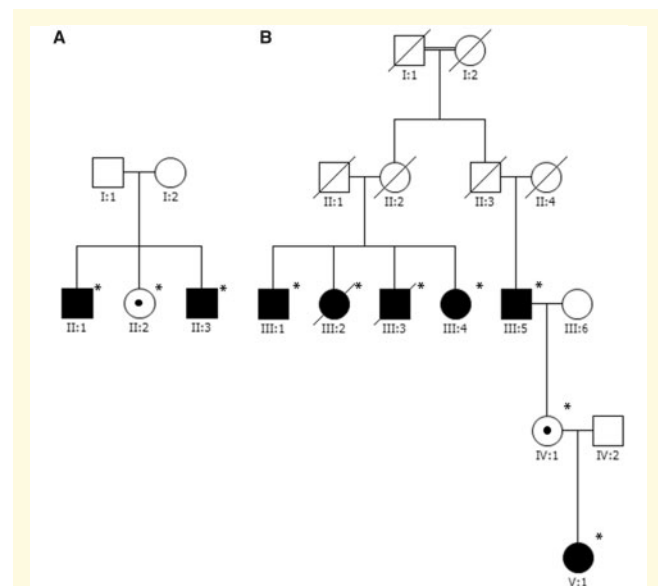


Figure 1 Pedigrees of the two multiplex families in the cohort. Asterisks indicate individuals that provided DNA for this study. A black circle inside the symbol of an unaffected individual indicates they are a CANVAS genotype carrier. (A) Family CII comprised Cook Island Māori individuals. (B) Family M2 comprised New Zealand Māori individuals. Although the first and second generations of family M2 were reported to be unaffected by their family, they were never formally assessed.

Genetic testing

To determine if affected individuals were homozygous for the CANVAS pathogenic repeat expansion, we followed the protocols described in *Cortese et al. (2019)*. Briefly, we performed standard PCR with primers flanking the CANVAS locus. The absence of any product suggests a homozygous expansion that is too large to be amplified by standard PCR. One band indicates that at least one allele is within the amplifiable range of normal PCR, and therefore the individual is not homozygous for a CANVAS pathogenic expansion. The expected product size is 355 bp, which corresponds to the reference (AAAAG)₁₁. A larger band indicates an intermediate sized expansion, larger than the reference allele but smaller than a full pathogenic expansion. For individuals where absence of a product upon flanking PCR suggested an expansion, we then performed repeat-primed PCR (RP-PCR), using primers specific for the AAAAG (reference allele), AAAGG (benign variant), and AAGGG (pathogenic) configurations. Because of Individual M2 V:1's unusually early clinical presentation, the Fulgent ataxia repeat expansion panel (*ATN1*, *ATXN1*, *ATXN10*, *ATXN2*, *ATXN3*, *ATXN7*, *ATXN8*, *ATXN8OS*, *BEAN1*, *CACNA1A*, *FMR1*, *FXN*, *NOP56*, *PPP2R2B*, *TBP*), and a broad neurogenetic gene panel (*Beecroft et al., 2020*) (genes are listed in [Supplementary Table 1](#)) were also performed to search for a possible other genetic condition explaining her early disease onset. In addition to these we performed functional studies to exclude Wilson's disease (copper studies), ataxia telangiectasia (alpha fetoprotein and ATM protein/kinase activity), vanishing white matter disease (transferrin isoforms) and white-cell enzyme testing.

Next-generation sequencing

Illumina whole genome sequencing (WGS) was performed on individuals CI1 II:1, C1 II:3, M2 III:4, and M2 V:1 via the Australian Genome Research Facility (Melbourne), following GATK4 (genome analysis tool kit version 4) best practices (*Poplin et al., 2018*). We compared this data against the selected markers from the haplotyping analysis by *Cortese et al. (2019)* (spanning chr4:38157510-40712481, hg19). Illumina whole exome sequencing (WES) was performed on Individuals M3 I:1, M4 I:1, M5 I:1, M6 I:1 and M7 I:1 via the Australian Genome Research Facility (Melbourne), following GATK4 best practices (*Poplin et al., 2018*). Using Linkdatagen (*Bahlo and Bromhead, 2009*), informative HapMap2 markers were extracted from the combined exome and genome sequencing and prepared for analysis with Merlin (*Abecasis et al., 2002*). Markers were excluded if they were covered to a read depth of <20-fold, or not sequenced in ≥50% of samples. We used Merlin to generate the most likely haplotypes. The length of the shared homozygous haplotype in centimorgans was calculated from the Merlin output. The haplotype lengths were used to calculate the most recent common ancestor assuming a 'correlated' genotype (95% confidence interval) using the Genetic Mutation Age Estimator tool (<https://shiny.wehi.edu.au/rafehi.h/mutation-dating/>) (*Gandolfo et al., 2014*), used in a recent haplotype analysis of CANVAS patients (*Rafehi et al., 2019*).

Data availability

Anonymised data are available from the corresponding author.

Results

Cohort

The summarized clinical features of the affected individuals are presented in [Table 2](#), which are compared with a cohort of 16 New Zealand European CANVAS patients (*Cortese et al., 2020*), and with the cohort published by *Cortese et al. (2019)*. Clinical features were similar across all three patient groups. Detailed clinical information for our cohort is shown in [Supplementary Table 1](#).

The mean age of symptom onset was 55 years (excluding Individual M2 V:1). The presenting neurological symptom was unsteadiness in all but one affected patient (Individual M2 III:4), where dysarthria predated unsteadiness by 2 years. Nine affected individuals described persistent cough, which predated neurological symptoms in three affected individuals. A third of patients complained of vestibular. In their initial neurological examination, seven affected individuals showed nystagmus. Ten affected individuals required a walker during their illness. The mean time between symptom onset and the use of a walking frame was 7 years (range 1–15 years). Two affected individuals died following study recruitment. Individual M2 III:5 experienced sudden cardiac death, but the cause of death for Individual M3 I:1 was unknown.

Investigations

Eight of 13 patients had electrodiagnostic studies. In six, motor nerve conduction studies were normal, and in two there was mild reduction in motor conduction velocity or amplitude. Nine affected individuals had cerebellar atrophy on initial MRI brain scan. Individual M2 III:4 had a normal brain MRI 3 years after symptom onset, but subsequent CT head scans showed cerebellar atrophy. Video head impulse tests were consistent with bilateral vestibulopathy in all 11 tested patients including those with a normal clinical head impulse test at initial neurological assessment. Individual M2 III:5 (*RFC1* pathogenic repeat positive) was asymptomatic at age 59 years, excepting chronic cough with syncope, and painful extremities. He showed mild bilateral vestibular impairment, but no further examinations were performed. He died from sudden cardiac death before he could be re-examined. Individuals M3 I:1, M4 I:1, M5 I:1 had formal autonomic nervous system testing. Abnormalities were inconsistently in the sympathetic and parasympathetic systems in different patients. Ultrasound examination showed small nerve cross-sectional areas in Individuals M4 I:1, M6 I:1, M7 I:1, but not Individual M2 V:1.

Individual M2 V:1

Of particular interest was individual M2 V:1. She presented at age 6 with tremor, gait unsteadiness, and learning difficulties. Tremor was reportedly present since infancy. Otherwise, motor milestones were normal. She had

Table 1 Summary of the pedigree and genetic information for the cohort

Family	Individual ID	Ethnicity	Affected	Flanking PCR product	RP-PCR		Result	NGS	Southern blot	
					AAGGG (pathogenic)	AAAAG (benign variation)			AAAAG (reference)	Allele size, kb
C11 Multiplex (Fig. 1A)	C11 II:1	Cook Island	Yes	–	+	+	Homozygous pathogenic	WGS	9470	1090
	C11 II:2	Māori	No	Intermediate size expansion	+	–	Carrier	–	NA	NA
M2 Multiplex (Fig. 1B)	C11 III:3		Yes	–	+	+	Homozygous pathogenic	WGS	NA	NA
	M2 III:1	Māori	Yes	–	+	–	Homozygous pathogenic	–	NA	NA
	M2 III:2		Yes	–	+	–	Homozygous pathogenic	–	NA	NA
	M2 III:3		Yes	–	+	–	Homozygous pathogenic	–	NA	NA
	M2 III:4		Yes	–	+	–	Homozygous pathogenic	–	NA	NA
	M2 III:5		Yes	–	+	–	Homozygous pathogenic	WGS	12 230/13 740	1640/1940
	M2 IV:1		No	Wild-type size band	+	+	Carrier	–	NA	NA
M3 Singleton	M2 V:1		Yes	–	+	–	Homozygous pathogenic	WGS	9000	990
M4 Singleton	M3 I:1	Māori	Yes	–	+	–	Homozygous pathogenic	WES	NA	NA
M5 Singleton	M4 I:1	Māori	Yes	–	+	–	Homozygous pathogenic	WES	NA	NA
M6 Singleton	M5 I:1	Māori	Yes	–	+	–	Homozygous pathogenic	WES	11 400	1480
M7 Singleton	M6 I:1	Māori	Yes	–	+	–	Homozygous pathogenic	WES	NA	NA
	M7 I:1	Māori	Yes	–	+	–	Homozygous pathogenic	WES	NA	NA

NGS = next-generation sequencing; RP-PCR = repeat-primed PCR; WES = whole exome sequencing.

Table 2 Comparison of clinical features in the different cohorts published

	Maori cohort <i>n</i> = 13	NZ European cohort <i>n</i> = 16	Cortese et al. (2019) <i>n</i> = 56 ^a
Mean age at symptom onset	55.4 ± 11 ^b	54.9 ± 12	54 ± 9
Time to first neurological assessment, years	4.0 ± 3.0	7.5 ± 7.2	11 ± 7
Gender, male (%)	8 (62)	6 (38)	27 (48)
Symptoms			
Cough (%)	8/10 (80)	6/9 (67)	21/56 (37)
Sensory symptoms (%)	7/13 (54)	8/16 (50)	N/A
Dysarthria (%)	10/13 (77)	8/16 (50)	N/A
Vestibular symptoms ^c (%)	3/9 (33)	5/16 (31)	N/A
REM sleep behaviour disorder (%)	2/5 (40)	7/10 (70)	N/A
Autonomic dysfunction ^b (%)	8/12 (67)	13/16 (81)	13/56 (23)
Signs at first neurological examination			
Ataxic gait (%)	12/12 (100)	15/16 (94)	45/56 (80) had cerebellar signs on examination, not further specified
Nystagmus (any direction) (%)	7/12 (58)	8/14 (57)	
Downbeat nystagmus (%)	5/11 (45)	5/14 (36)	
Limb ataxia (upper or lower) (%)	9/11 (82)	9/14 (64)	
Positive head impulse test (%)	4/6 (67)	11/11 (100)	30/56 (53)
Reflexes (%)			
Reduced	7/12 (58)	9/16 (56)	N/A
Normal	5/12 (42)	4/16 (25)	
Brisk	–	3/16 (19)	
Sensory loss (any modality) (%)	7/11 (64)	12/14 (86)	56/56 (100)
Time to walking frame, years	11 ± 7.6	5.9 ± 6.0	N/A
Investigations			
Small or absent SNAPs (%)	8/8 (100)	15/15 (100)	56/56 (100)
Small cross-sectional area on nerve ultrasound (%)	3/3 (100)	6/7 (86)	N/A
MRI or CT vermal atrophy (%)	9/10 (91)	15/16 (94)	35/42 (83)
vHIT abnormal (%)	9/10 (90) ^d	15/16 (94)	N/A

Comparison of clinical features of Cook Island and New Zealand Māori patients with the New Zealand European cohort described in Cortese et al. (2020), and the European cohort described by Cortese et al. (2019). For New Zealand cohorts, denominators are the number of patients for whom a symptom or sign is documented. Symptoms refers to patient reported symptoms at any point during the course of illness. Autonomic dysfunction refers to either symptoms of autonomic dysfunction or abnormal autonomic function testing. SNAPs = sensory nerve action potentials; vHIT = video head impulse test.

^aUK Cohort published by Cortese et al. (2019).

^bExcludes Individual M2 V:1.

^cOscillopsia or visual blurring or dizziness on head turning.

^dOne additional patient (Individual M2: III:5) had borderline changes.

prominent upper limb intention tremor and impaired tandem gait. Communication was significantly impaired by dysarthria. Cognition was difficult to assess formally. She had no nystagmus or sensory deficit, but upper neuron signs with increased tone and extensor plantars. Brain MRI at age 6 showed increased signal in the cerebellar peduncles and dorsal brainstem (Supplementary Fig. 2A). A limited follow-up scan at the age of 15 showed particular prominence of the horizontal fissure, as is seen in crus 1 cerebellar atrophy of CANVAS, together with enlarged supratentorial CSF spaces consistent with a degree of more widespread atrophy (Supplementary Fig. 2B). The scan was limited because of movement so the white matter changes seen previously were unable to be interrogated further. She was wheelchair-bound at age 8. At age 20, she additionally showed profound limb ataxia as measured using the finger-nose-finger, finger chase and heel shin tests of the scale for the assessment and rating of ataxia (SARA); her SARA score was 31. Bilateral vestibular failure was demonstrated on video head impulse test, with a gain of 0.46 (left) and 0.49 (right). Nerve conduction

studies (age 20) were atypical for CANVAS showing mild, uniform slowing of conduction velocities but normal sensory and motor nerve amplitudes. Extensive investigation for other causes of ataxia (including Friedreich's ataxia) and cognitive impairment revealed no alternative cause. The neurogenetic gene panel and Fulgent ataxia panel revealed no likely pathogenic variants, and all functional testing was normal.

Flanking PCR

There was no PCR product in 13/15 individuals (Table 1), indicating they harboured an expansion on both alleles. Of the two remaining individuals, Individual M2 IV:1 showed a ~355 bp band, indicating one normal-sized allele. Individual CI1 II:2 showed a larger band, indicating an intermediate sized allele that was expanded. All affected individuals had no PCR amplifiable product, while the two unaffected individuals did show a PCR product. Thus, the expanded allele segregated with disease.

Repeat-primed PCR

All 13 individuals without a band on flanking PCR were also negative on repeat-primed PCR for the reference pentanucleotide sequence (AAAAG) at the CANVAS locus. These individuals showed the pathogenic AAGGG repeat, as seen in the European CANVAS population (Fig. 2B). However, they were also found to have a novel configuration at the locus. The pathogenic AAGGG expansion was preceded by a stretch of AAAGG benign variant repeats (Fig. 2B), which varied in number. The individuals had the conformation $(AAAGG)_{10-25}(AAGGG)_{exp}$. The carriers Individuals M2 IV:1 and CI1 II:2 each harboured one allele of this configuration. On the other allele, Individual M2 IV:1 had the reference sequence $(AAAAG)_{11}$, while Individual CI1 II:2 had an intermediate sized AAAGG expansion.

Next-generation sequencing

Visual interrogation of soft-clipped reads in the BAM files of the WGS for Individuals CI1 II:2, M2 III:2, and M2 IV:1 showed a small number of repeats of the benign variant allele $(AAAGG)_{4-6}$ at the distal end of the *RFC1* pathogenic expansion in the reads that covered this region (Fig. 2C). The coverage of this region in Individual CI1 II:1 was too low to reliably detect this pattern. The disease-associated repeat expansion in the Māori and Cook Island Māori is thus a hybrid allele of the pathogenic AAGGG repeat embedded in benign variant AAAGG repeats (Fig. 2A).

Haplotype analysis

Cortese *et al.* (2019) identified a shared haplotype in their patients, encompassing a 47.9 kb core region that was identical in all but one patient (chr4:39318706-39366590, hg19). Our four patients with WGS data shared this core haplotype, plus an additional region extending from chr4:39122697-39366590 (0.24 Mb total shared) (Supplementary Table 2). We then combined the WES and WGS data to impute the most likely haplotypes for our patients (Supplementary Table 3). This showed an extended shared haplotype in our cohort, spanning chr4:36317970-44295839 (7.98 Mb; Supplementary Table 3). Based on the length of the shared haplotype in centimorgans, the estimated most recent common ancestor was 25.6 generations ago (95% confidence interval 11.1–60.7). Assuming that one generation is 25 years, the most recent common ancestor was 650 years ago (95% confidence interval 275–1525; dating to 1369 CE, 95% confidence interval 494–1744 CE). Assuming instead that one generation is 20 years, this would place the most recent common ancestor 520 years ago (95% confidence interval 220–1200 years; dating to 1499 CE, 95% confidence interval 819–1799 CE).

By combining the analysis of the Cortese *et al.* (2019) haplotype age with our four WGS patients, we were able to estimate the most recent common ancestor for the combined cohort. Assuming a correlated genealogy, the mutation arose

1518.5 generations ago (95% confidence interval 65.9–2942.5). Assuming one generation is 20 years, the mutation is 30380 years old (95% confidence interval 132–58860). Assuming 25 years, 37975 years old (95% confidence interval 1650–73575). This suggests there was a distant common ancestor for both the Māori/Cook Island and Caucasian patients.

Southern blot

Southern blot of two affected Cook Island heritage and one Māori patient (Individuals CI1 II:1, M2 III:4, M2 V:1 and M5 I:1), showed expanded alleles as described by Cortese *et al.* (2019), with two distinct bands in an individual carrying expansions of different sizes, or one band, or a thick band if the expanded alleles had a similar size. The allele size and number of repeated units are detailed in Table 1. The Southern blot image is shown in Supplementary Fig. 1.

Discussion

Our results demonstrate that the *RFC1* pentanucleotide repeat expansion described by Cortese *et al.* (2019) is responsible for CANVAS in a non-Caucasian population. We also show a novel configuration of the CANVAS pathogenic pentanucleotide repeat, which appears to be specific to the Māori population. Despite the difference in repeat configuration, there were no apparent phenotypic differences between this cohort and New Zealand European or international cohorts. However, the small sample size ($n = 13$) limits the ability to detect differences.

The rapid childhood onset presentation of Individuals M2 V:1 may represent a variant, early onset form of the disease, as seen in other typically late onset repeat expansion disorders such as Huntington's disease (Cronin *et al.*, 2019) or SCA-7 (Benton *et al.*, 1998). M2 V:1 has two of the three clinically defining features of CANVAS: ataxia and bilateral vestibular failure. Co-occurrence of these features is highly distinctive of CANVAS (having excluded Friedreich's ataxia). The normal nerve cross-sectional area seen in this patient has also been previously described in a CANVAS cohort (Pelosi *et al.*, 2017). Although, until we understand fully the pathogenesis of CANVAS and can test for biomarkers of that, the possibility of a second condition cannot be excluded.

We report rapid eye movement sleep behaviour disorder as a feature of CANVAS for the first time, occurring in both our New Zealand European and Māori patients (Table 2). This was so prominent in one European patient that the diagnosis of multiple systems atrophy was initially entertained, but later excluded.

The 0.24 Mb core shared haplotype between our cohort and that of Cortese *et al.* (2019) supports the single origin of the CANVAS disease allele, as suggested by Rafahi *et al.* (2019). There appears to be a relatively recent founder effect in the Māori population. The most recent common ancestor of this cohort is estimated to date to ~650–520 years ago

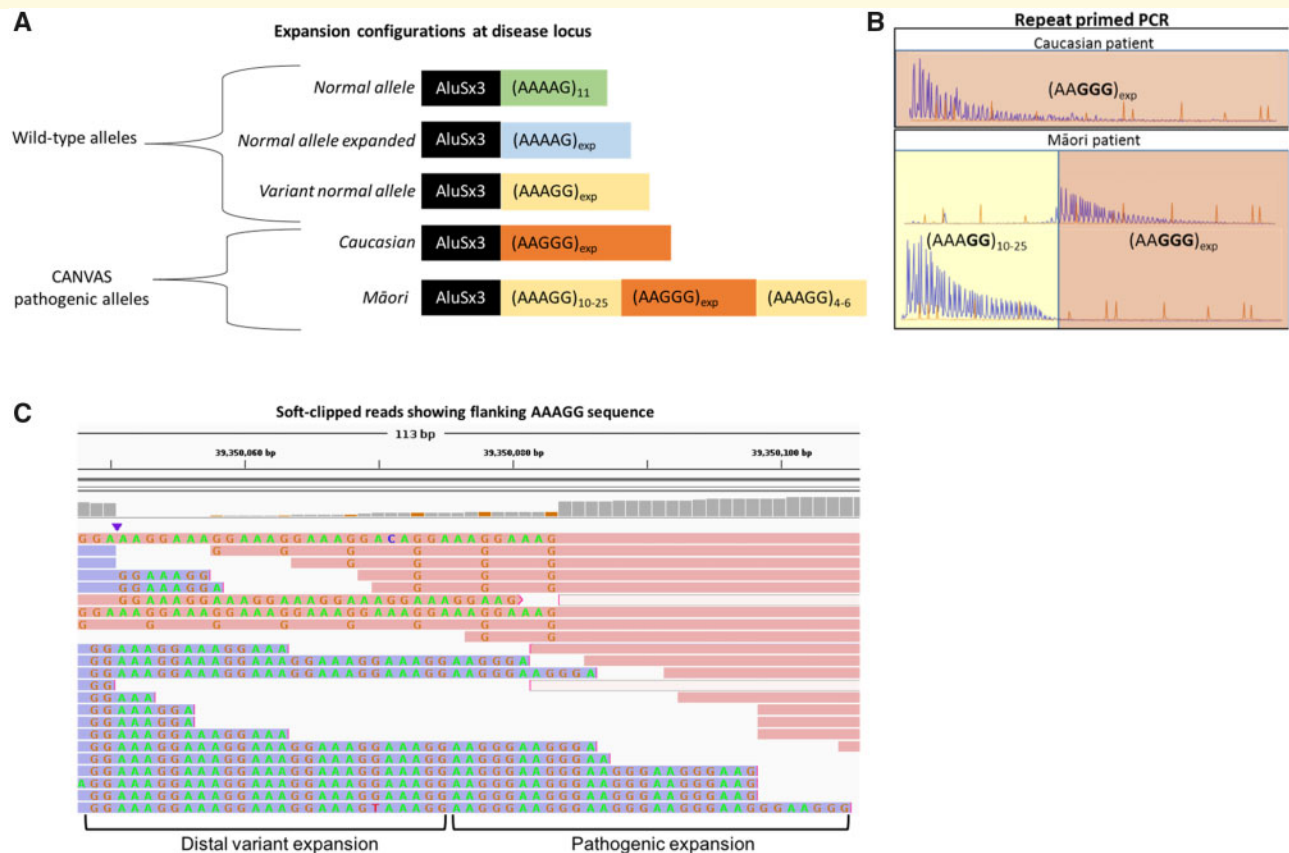


Figure 2 Summary of *RFC1* configurations. (A) Schematic representation of the repeat alleles at the CANVAS locus, demonstrating the non-pathogenic alleles (top) and the pathogenic alleles (bottom). (B) Representative repeat-primed PCR results demonstrating the new CANVAS configuration. The typical *RFC1* (AAGGG)_{exp} repeat pattern is seen in a Caucasian CANVAS patient (top). The novel configuration of (AAAGG)₁₀₋₂₀(AAGGG)_{exp} is shown below. The few (AAAGG) repeats at the distal end of the *RFC1* pathogenic expansion were not seen with the repeat-primed PCR. (C) Representative soft-clipped reads from WGS BAM file, showing the presence of a small number of AAAGG repeats that are continuous with the distal end of the pathogenic AAGGG repeat.

(i.e. ~1370–1500 CE). This estimated time period roughly overlaps with the Māori settlement of New Zealand [~1250–1300 CE (Wilmshurst *et al.*, 2008)]. If this allele was present early in the Māori settlement of New Zealand, CANVAS may be especially prevalent in individuals of Māori descent. Further genetic characterization of the Māori population would be required to define the allele frequency, and epidemiological studies are required to assess the CANVAS disease burden within this population.

Although variation in the number of repeated units is common (Paulson, 2018), the discovery of this variable repeat configuration is highly unusual for a repeat-expansion disease. AAGAG and AGAGG configurations have been described, but it is unknown if they are definitively pathogenic (Akçimen *et al.*, 2019). Cortese *et al.* (2019) suggested the expansion size is correlated with GC content, with the AAGGG configuration allowing a larger expansion to form. The (AAAGG)₁₀₋₂₅ expansion preceding the large AAGGG expansion supports this. The 3% of Caucasian patients from Cortese *et al.* (2019) who had an uncharacterized expansion at the *RFC1* disease locus suggest additional pathogenic configurations will be discovered in time. It will be

interesting to see if any novel pathogenic repeat expansions at the *RFC1* locus are population specific or share a core haplotype (Cortese *et al.*, 2019; Rafehi *et al.*, 2019).

Acknowledgements

We sincerely thank the patients and their families for their participation in this study. We thank Dr Bharti Morar for her insight on the haplotype analysis. Additional acknowledgement is made to New Zealand neurologists, Drs Neil Anderson, Peter Bergin, Andrew Chancellor, Nick Cutfield, David Hutchinson, Elizabeth Walker, Mark Simpson and Barry Snow all of whom referred patients to this study and without whose clinical acumen it would not have been possible. We also thank Dr David Perry for providing the MRI images.

Funding

S.J.B. is funded by The Fred Liuzzi Foundation (TFLF) (Melbourne, Australia). A.C. is funded by Medical Research Council (MR/T001712/1), Wellcome Trust (204841/Z/16/Z)

and the Inherited Neuropathy Consortium (INC), which is a part of the NIH Rare Diseases Clinical Research Network (RDCRN) (U54NS065712). H.H. and M.M.R. are grateful to the Medical Research Council (MRC), MRC Centre grant (G0601943), and M.M.R. is also grateful to the National Institutes of Neurological Diseases and Stroke and office of Rare Diseases (U54NS065712) for their support. H.H. is also supported by Ataxia UK, The MSA Trust, MDUK and The Muscular Dystrophy Association (MDA). M.M.R. is supported by the National Institute for Health Research University College London Hospitals Biomedical Research Centre. The views expressed are those of the author(s) and not necessarily those of the NHS, the NIHR or the Department of Health. N.G.L. (APP1117510) and G.R. (APP1122952) are supported by the Australian National Health and Medical Research Council (NHMRC). G.R. is also supported by a Western Australian Department of Health Future Health's WA Merit Award. This work is funded by TFLF and NHMRC (APP1080587). The funding agencies were not involved in the design, completion, or writing of this study.

Competing interests

The authors report no competing interests.

Supplementary material

Supplementary material is available at *Brain* online.

References

- Abecasis GR, Cherny SS, Cookson WO, Cardon LR. Merlin-rapid analysis of dense genetic maps using sparse gene flow trees. *Nat Genet* 2002; 30: 97–101.
- Akçimen F, Ross JP, Bourassa CV, Liao C, Rochefort D, Gama MTD, et al. Investigation of the RFC1 repeat expansion in a Canadian and a Brazilian ataxia cohort: identification of novel conformations. *Front Genet* 2019; 10: 1219.
- Bahlo M, Bromhead CJ. Generating linkage mapping files from Affymetrix SNP chip data. *Bioinformatics* 2009; 25: 1961–2.
- Beecroft SJ, Yau KS, Allcock RJN, Mina K, Gooding R, Faiz F, et al. Targeted gene panel use in 2249 neuromuscular patients: the Australasian referral center experience. *Ann Clin Transl Neurol* 2020; 7: 353–62.
- Benton CS, de Silva R, Rutledge SL, Bohlega S, Ashizawa T, Zoghbi HY. Molecular and clinical studies in SCA-7 define a broad clinical spectrum and the infantile phenotype. *Neurology* 1998; 51: 1081–6.
- Cortese A, Simone R, Sullivan R, Vandrovicova J, Tariq H, Yan YW, et al. Biallelic expansion of an intronic repeat in RFC1 is a common cause of late-onset ataxia. *Nat Genet* 2019; 51: 649–58.
- Cortese A, Tozza S, Yau WY, Rossi S, Beecroft SJ, Jaunmuktane Z, et al. Cerebellar ataxia, neuropathy, vestibular areflexia syndrome due to RFC1 repeat expansion. *Brain* 2020; 143: 480–90.
- Cronin T, Rosser A, Massey T. Clinical presentation and features of juvenile-onset Huntington's disease: a systematic review. *J Huntingtons Dis* 2019; 8: 171–9.
- Gandolfo LC, Bahlo M, Speed TP. Dating rare mutations from small samples with dense marker data. *Genetics* 2014; 197: 1315–27.
- Paulson H. Repeat expansion diseases. In: Geschwind DH, Paulson HL, Klein C, editors. *Handbook of clinical neurology*. Amsterdam: Springer Berlin Heidelberg; 2018. p. 105–123.
- Pelosi L, Leadbetter R, Mulroy E, Chancellor AM, Mossman S, Roxburgh R. Peripheral nerve ultrasound in cerebellar ataxia neuropathy vestibular areflexia syndrome (CANVAS). *Muscle Nerve* 2017; 56: 160–2.
- Pelosi L, Mulroy E, Leadbetter R, Kilfoyle D, Chancellor AM, Mossman S, et al. Peripheral nerves are pathologically small in cerebellar ataxia neuropathy vestibular areflexia syndrome: a controlled ultrasound study. *Eur J Neurol* 2018; 25: 659–65.
- Poplin R, Ruano-Rubio V, DePristo MA, Fennell TJ, Carneiro MO, Auwera GVD, et al. Scaling accurate genetic variant discovery to tens of thousands of samples. *bioRxiv* 2018: 201178.
- Rafehi H, Szmulewicz DJ, Bennett MF, Sobreira NL, Pope K, Smith KR, et al. Bioinformatics-based identification of expanded repeats: a non-reference intronic pentamer expansion in RFC1 causes CANVAS. *Am J Hum Genet* 2019; 105: 151–65.
- Szmulewicz DJ, McLean CA, Rodriguez ML, Chancellor AM, Mossman S, Lamont D, et al. Dorsal root ganglionopathy is responsible for the sensory impairment in CANVAS. *Neurology* 2014; 82: 1410–5.
- Szmulewicz DJ, Waterston JA, Halmagyi GM, Mossman S, Chancellor AM, McLean CA, et al. Sensory neuropathy as part of the cerebellar ataxia neuropathy vestibular areflexia syndrome. *Neurology* 2011; 76: 1903–10.
- Taylor JM, Snow BJ, Roxburgh RH, Bergin PS, Chancellor AM, Cleland JC, et al. Autonomic dysfunction is a major feature of cerebellar ataxia, neuropathy, vestibular areflexia 'CANVAS' syndrome. *Brain* 2014; 137: 2649–56.
- Wilmshurst JM, Anderson AJ, Higham TFG, Worthy TH. Dating the late prehistoric dispersal of Polynesians to New Zealand using the commensal Pacific rat. *Proc Natl Acad Sci USA* 2008; 105: 7676–80.